

Activated Carbon from Bio-wastes of Durian Fruits as Active Material for Electrodes of Electric Double-layer Capacitors

J.P. Tey¹, A.K. Arof¹, M.A. Yarmo², and M.A. Careem^{1,*}

¹Centre for Ionics University of Malaya, Department of Physics, Faculty of Science, University of Malaya, 50603 Kuala Lumpur, Malaysia

²School of Chemical Sciences & Food Technology, Faculty of Science & Technology, National University of Malaysia, 43600 Bangi, Selangor, Malaysia

Received: September 01, 2015, Accepted: October 01, 2015, Available online: December 28, 2015

Abstract: In this study, bio-wastes from durian fruits such as seeds and shells have been used as precursor materials to prepare activated carbon (AC). While the applicability of a one-step method of impregnation-activation has been investigated for the activation of durian shells, a two-step method of carbonization-impregnation-activation has been tried for the durian seeds. Durian shells based AC (DSh-AC) was found to have a BET surface area (S_{BET}) of $2004 \text{ m}^2 \text{ g}^{-1}$ and the durian seeds based AC (DS-AC) had S_{BET} of $1176 \text{ m}^2 \text{ g}^{-1}$. A new approach to electrical double-layer capacitor (EDLC) fabrication has been attempted to avoid the use of polymer binders and organic solvents in the electrodes by coating the electrode material directly on the separator. Instead of coating onto metal current collector, the AC was coated on a glass microfiber filter which was used as the separator to form the electrode. As an electrode material in the EDLC, DSh-AC performed well with a specific capacitance (C_{SC}) between 72 and 82 F g^{-1} whereas the DS-AC showed lower values of C_{SC} between 64 and 70 F g^{-1} . The reasonable good results indicate that the simple approach of device fabrication can also produce EDLCs with satisfactory performance parameters.

Keywords: durian; bio-waste; activated carbon; electrode material; electric double-layer capacitor

1. INTRODUCTION

Conventional capacitors store electrical energy by accumulating charges at the electrodes using the electrostatic principle. In such capacitors, two electrical conductors are separated by a thin layer of dielectric material. A potential difference applied between these conductors generates an electrical field across the dielectric causing the positive charges to accumulate near one conductor and negative charges near the other conductor. Charge storage ability of capacitors is measured in terms of capacitance which is proportional to the thickness of the dielectric, surface area of the conductors, and the potential difference between the conductors.

Electric double-layer capacitors (EDLCs) are an evolution from the conventional capacitors. In EDLCs, electrodes made with a highly porous material are separated by a porous insulator soaked in a liquid electrolyte. The high porosity of the electrodes gives rise to high surface area. When a potential difference is applied between the two electrodes, electrons will move out from one of

the electrodes and enter into the other electrode. Hence, an electric field is induced between the electrodes. Cations and anions of the electrolyte will be drawn to the negative and positive electrodes respectively, forming two analogous capacitors in series. The charge separation between the charges on the electrode surface and the electrolyte occurs at the molecular level. The high surface area of the electrodes and very small double charge layer thickness result in very large capacitance.

Activated carbon (AC) was the first electrode material used in the development of EDLCs. It has high porous nature and also high surface area. As AC is inert to chemicals, long cycle life for EDLCs can be expected. Numerous research works on the electrode materials of EDLC were reported [1-6]. Addition of metal oxides into the AC electrodes or employment of metal oxides themselves as electrodes produces high pseudocapitance which is useful to produce pseudocapacitors [7-10]. Hybrid EDLCs which utilize asymmetric electrodes with cathodes made with traditional AC and anodes with battery-like electrode were also reported [11, 12]. AC is still a favourable electrode material for

*To whom correspondence should be addressed: Email: macareem@um.edu.my
Phone: +603 7967 4093

EDLCs because of the simple fabrication procedures, relatively low production cost and the abundance of carbon sources [13-15]. Agricultural wastes such as palm shells, coconut shells, rice husks and straws, and even mangosteen (*Garcinia mangostana*) shells had been widely investigated as carbonaceous precursors of AC [16-19].

The first goal of this study focuses on the preparation of AC from seeds (DS) and shells (DSh) of durian as electrode material for EDLCs. Activation method is the key in controlling the pore characteristics of the AC surface. Chemical activation is favoured over physical activation mainly because of the relatively lower pyrolysis temperature and relatively higher yield of AC [20, 21]. Different preparation methods of AC from DSh have been tried previously by researchers using carbon dioxide, potassium hydroxide, and sodium hydroxide as activating agents [22-24]. In another study, preparation of AC from DS using phosphoric acid as the activating agent has been reported [25]. In the work reported here, DS are carbonized into char first. This DS char will be impregnated with potassium hydroxide and activated. As for DSh, it will be directly impregnated with phosphoric acid and then activated. As far as the authors are aware, no such procedures have been reported in the literature. The above described different activation method was used for DSh because the carbonization method did not give good yield.

The second part of this study is a new attempt on the fabrication method of EDLC electrode. The widely used form of electrode is made by coating the AC slurry on a metal foil or mesh. The typical methods include blade coating, dip coating, and spray coating. In order to make the slurry adhere onto metal, polyvinylidene difluoride (PVDF) is normally used as the binder which requires an organic solvent like N-methyl-2-pyrrolidone (NMP) for dissolution. In our case, the AC slurry will be coated on the porous separator rather than on the metal current collector, using a water-based binder made with carboxymethyl cellulose (CMC). A direct coating onto the metal current collector cannot ensure a good adhesion as the dried coating will easily crack and peel off by itself. The separator allow slurry to flow into its porous network and a layer of electrode is formed after drying. Here, a glass microfiber filter (GMF) will serve as the separator. Sodium sulfate (Na_2SO_4) which is widely used as an electrolyte for EDLCs due to its higher potential stability window [26, 27] will be used as the electrolyte in this study.

2. EXPERIMENTAL

2.1. Materials

Durio zibethinus is one of the durian species which is edible and commonly available in the international market. In Malaysia, durian is consumed as a favourite fruit by the locals and it is available all year round with large quantities available during the fruiting season [28]. The flesh which constitutes approximately one-third of the mass of the fruit is the only edible part and all other parts are disposed as wastes. From 2008 to 2010, about 90000 metric tons of durian wastes were generated annually from the durian industry [29]. Durian shells have no commercial use so far and are disposed after the extraction of the flesh with seeds. Based on past studies of ultimate analysis, DS have 47.32 wt% of carbon and DSh have 60.31 wt% of carbon [22, 25]. This study is an attempt to find use for these waste products by converting them to AC with high porosity.

2.2. Physical characterization of ACs

A thermal analyzer (TA Instruments TGA Q500) was used to determine the thermal decomposition temperature T_d of durian seeds and shells. The sample was heated from room temperature to 800 °C at a rate of 50 °C min^{-1} under N_2 flow of 40 ml min^{-1} . The TG profile could also provide information about when decomposition had stopped. The surface morphologies of DS-AC and DSh-AC were observed with a field emission-scanning electron microscope (FE-SEM) JEOL JSM-7600F. X-ray diffractograms of the ACs were obtained to check whether the characteristic peaks of AC appear at diffraction angles (2θ) 26° and 43° or not. The XRD measurements were made with tabletop inXitu BTX-II which uses a CuK_α source under operating voltage and current of 30.0 kV and 1.0 mA, respectively. Porosimetry analyzer (Micromeritics ASAP 2020) was used to evaluate the pore structure of the prepared ACs through N_2 adsorption-desorption done at -196 °C. The sorption isotherm data served as raw data for the interpretation of AC properties. Brunauer-Emmett-Teller (BET) model was used to determine the BET surface area (S_{BET}). Microporous surface area (S_{mic}), external surface area (S_{ext}), and microporous volume, (V_{mic}) were determined by t -plot method.

2.3. Preparation of ACs

Seeds and shells of durian fruits were collected from disposal sections of local durian stalls and were washed with water to remove most of the impurities like flesh and dirt. The cleaned seeds and shells were then air-dried and heated in an oven at 110 °C for 24 hours to remove the water content. After drying, they were ground into granules of size approximately less than 2.0 mm. The durian seeds granules (DS) and durian shells granules (DSh) were kept in an airtight container for the preparation of AC.

The carbonization of DS was carried out in a tube furnace (Jisico J-GAF-H) by heating from room temperature to 700 °C at a rate of 10 °C min^{-1} and maintaining at 700 °C for 30 minutes. During the heating process, 1.0 liter min^{-1} flow of nitrogen gas (N_2) was introduced in the furnace to avoid combustion of the DS. The carbonized DS (cDS) were left to cool until the temperature reached 50 °C and then they were mixed with potassium hydroxide (KOH) pellets in 1:1 weight ratio. 75 ml of distilled water was added into the mixture to form an impregnation mixture while being agitated continuously for 24 hours. The impregnation mixture was left in the oven at 110 °C for 24 hours to allow evaporation of any water present. The impregnated cDS was pyrolyzed with the same heating profile and N_2 flow but maintained at 700 °C for 60 minutes instead of 30 minutes.

On the other hand, DSh were directly impregnated in 1.0 M phosphoric acid with a 1:25 mass to volume ratio. The solid-liquid mixture was agitated for 24 hours and left in the oven at 110 °C for 24 hours to evaporate the water present. This impregnated DSh was pyrolyzed at 700 °C for 60 minutes after heating from room temperature at a rate of 10 °C min^{-1} under 1.0 liter min^{-1} flow of N_2 .

The end products, durian seeds based AC (DS-AC) and durian shells based AC (DSh-AC) were washed with hot hydrochloric acid followed by 8 rounds of washing with distilled water until the pH level reached neutral. The washed DS-AC and DSh-AC were dried in the oven at 110 °C for 24 hours. They were then ball-milled for 24 hours to form powder suitable for characterizations and preparation of electrodes.

2.4. Preparation of electrode and fabrication of EDLC

For the construction of EDLC, two types of slurry were prepared by mixing the as-prepared DS-AC and DSh-AC separately with carboxymethyl cellulose (CMC) as binder and carbon black as electrical conducting additive in the weight ratio of 87:9:4. Distilled water was used as the solvent for the formation of slurry under prolonged agitation. The slurry was spread onto one side of the glass microfiber (GMF) and left for drying under ambient condition for 24 hours. A small amount of graphite was smeared onto the coated side of the GMF to enhance the electrical contact with the stainless steel current collector. The uncoated side of the GMF was then wetted with the electrolyte, 1.5 M of sodium sulfate (Na_2SO_4). Two identical slurry coated and electrolyte impregnated GMFs were joined together with the uncoated sides facing each other and sandwiched between two stainless steel cell plates to form the EDLC.

2.5. Electrochemical characterization of EDLC

Cyclic voltammetry (CV) was performed using a Metrohm Autolab PGSTAT204 by applying a forward and reverse linear potential scan to the EDLC cell and measuring the current as a function of time and the results obtained are presented as voltammograms of current against potential. Capacitance for the EDLC (C_{EDLC}) was calculated with Equation (1) using the data from the cyclic voltammograms. The specific capacitance of the single electrode (C_{sc}) was calculated by Equation (2).

$$C_{EDLC} = (s \cdot V)^{-1} \int I(V) dv \quad (1)$$

where s is scan rate (Vs^{-1}), V is instantaneous potential during discharge of EDLC, and $I(V)$ is the current at potential V .

$$C_{sc} = \frac{2C_{EDLC}}{m} \quad (2)$$

where m is mass of the electrode material of a single electrode (g).

Impedance spectrum of the EDLC was measured in the frequency range of 10 mHz to 100 kHz with an *a.c.* signal of amplitude of 0.1 V and interpreted using Nyquist plots (imaginary Z'' against real Z'). The $Z' C_{sc}$ can be C_{sc} evaluated using the Z'' imaginary data of the lowest frequency available which is 10 mHz. C_{sc} is calculated by Equation (3).

$$C_{sc} = -\frac{2}{2\pi \cdot 0.01 \cdot Z''} \cdot \frac{1}{m} \quad (3)$$

The stability of the EDLCs were tested using galvanostatic charge-discharge for 1000 cycles at 5.0 mA between 0.1 V and 1.0 V. Data was recorded as potential as a function of time. Equation (4) was used to calculate C_{sc} .

$$C_{sc} = 2 \cdot \frac{I}{m} \cdot \frac{\Delta t}{\Delta V} \quad (4)$$

where I is constant current at discharge, m is mass of the electrode material in a single electrode, Δt is discharge time, and ΔV is potential difference of discharge.

The energy density (E), power density (P), and Coulombic effi-

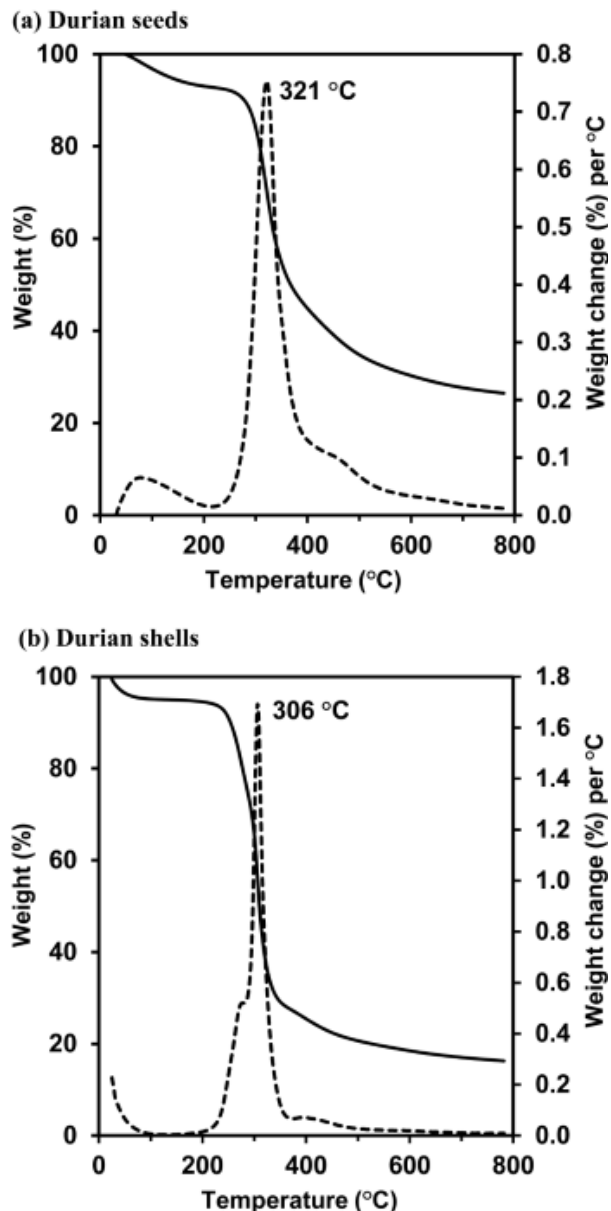


Figure 1. TG profiles of (a) raw durian seeds and (b) raw durian shells. Complete line depicts the weight percentage while dotted line depicts the weight change per unit temperature change.

ciency (η) of the EDLC were calculated using Equation (5), Equation (6), and Equation (7) respectively.

$$E = \frac{1}{2} \cdot C_{sc} (\Delta V)^2 \cdot \frac{1000}{3600} \quad (5)$$

$$P = \frac{I \cdot \Delta V}{2m} \cdot 1000 \quad (6)$$

$$\eta = \frac{\Delta t_d}{\Delta t_c} \cdot 100\% \quad (7)$$

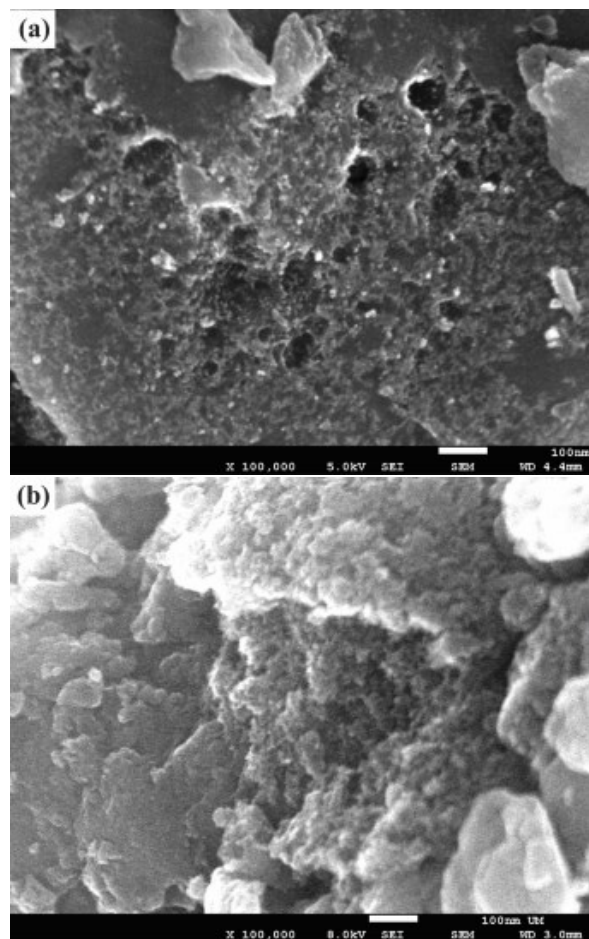


Figure 2. FE-SEM images of (a) DS-AC and (b) DSh-AC.

where Δt_d is discharge time and Δt_c is charge time.

All the EDLC characterizations were done at room temperature.

3. RESULTS AND DISCUSSION

3.1. Physical properties of ACs

Figure 1(a) and 1(b) show the thermogravimetric (TG) profiles of DS and DSh respectively. The rapid decompositions of DS and DSh give sharp mass losses at 321 and 306 °C respectively. The decomposition is mainly attributed to the carbonization of the precursor where volatile matters such as carbon dioxide, nitrogen and even some hydrocarbons are released. At temperatures above 400 °C, the minute mass loss is due to the further discharge of residual volatile matters. Hence, 700 °C was chosen as the temperature for carbonization or activation because most of the volatile matters and tar would have been released from the raw materials resulting in carbon material with better porous structure.

FESEM micrographs shown in Fig. 2 reveal the surface morphologies of activated carbons. The evolution of volatile matters and diffused chemicals during activation created random large pores of various sizes on the outer surface. The formation of pores not only ensures higher surface area but also provides access to interior of the material. Due to the limitation of FESEM, macropores (>50

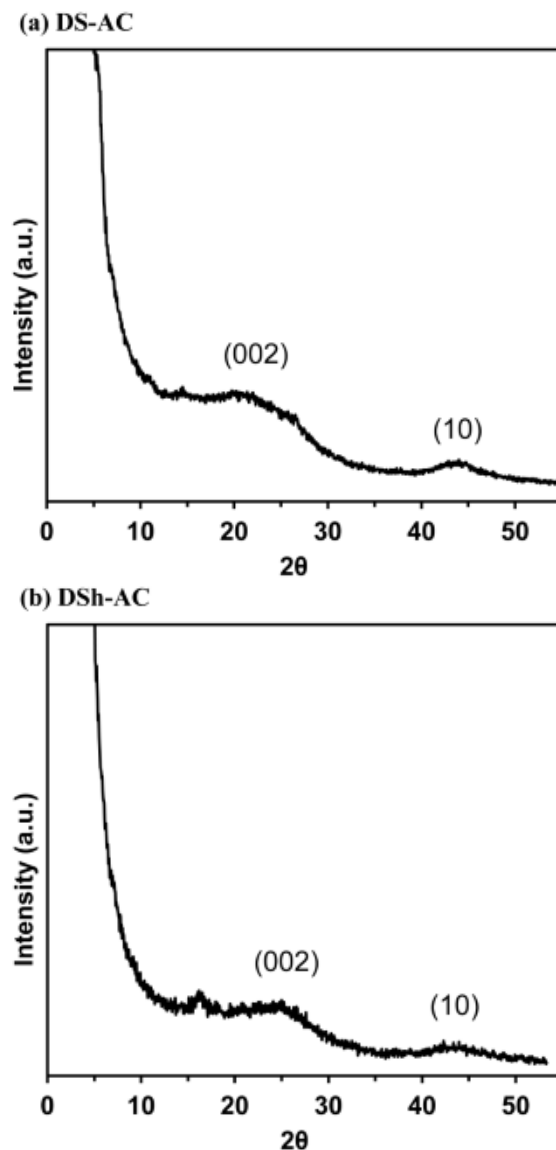


Figure 3. X-ray diffractograms of (a) DS-AC and (b) DSh-AC.

nm) and mesopores (between 2 and 50 nm) were only observed visually. The sizes of the pores are classified according to International Union of Pure and Applied Chemistry (IUPAC) classification [30].

X-ray diffractograms (XRD) of the prepared ACs shown in Fig. 3 exhibit two characteristic AC broad peaks. The broad peaks at diffraction angles $2\theta \sim 23^\circ$ and $\sim 43^\circ$ correspond to the disordered

Table 1. Porosity parameters of DS-AC and DSh-AC.

Sample	S_{BET}^a	S_{mic}^b	S_{ext}^c	V_t^d	V_{mic}^e	D^f
DS-AC	1176	753	423	0.569	0.346	1.93
DSh-AC	2004	60	1944	1.58	0.04	3.34

^{a)} BET surface area ($m^2 g^{-1}$); ^{b)} microporous surface area ($m^2 g^{-1}$); ^{c)} external surface area ($m^2 g^{-1}$); ^{d)} total pore volume ($cm^3 g^{-1}$); ^{e)} microporous volume ($cm^3 g^{-1}$); ^{f)} average pore width (nm).

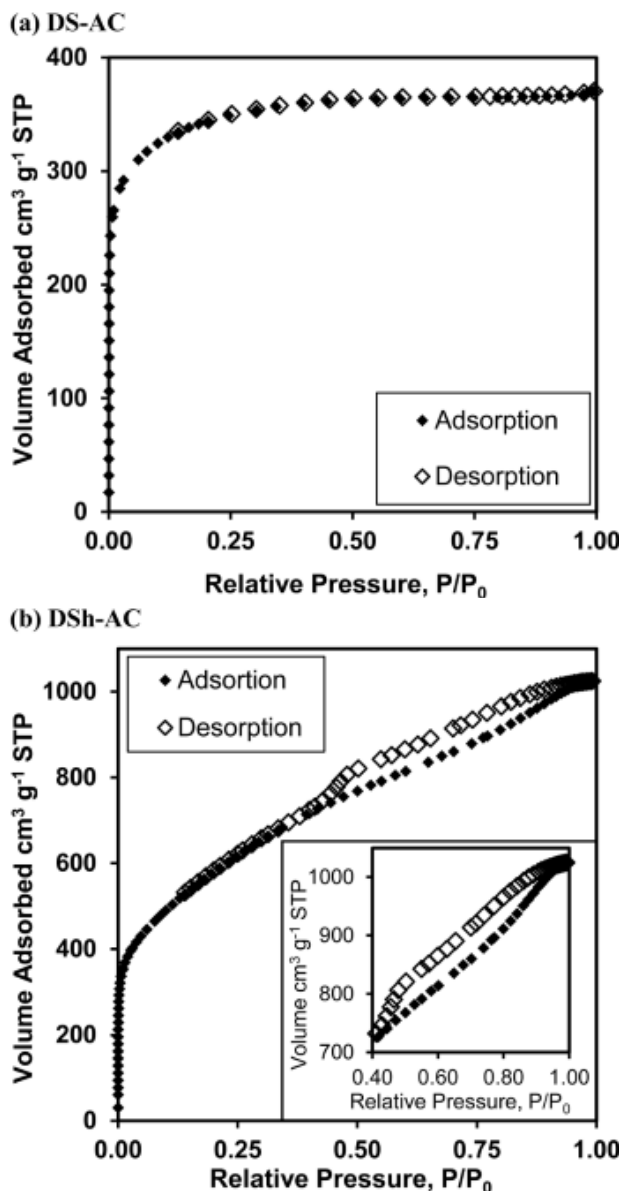


Figure 4. Adsorption/desorption isotherms of N_2 at $-196^\circ C$ for (a) DS-AC and (b) DSh-AC. The inset in (b) shows the hysteresis.

graphitic (002) and (10) planes respectively [31]. (10) plane is the overlapping of (100) and (101) planes. The small peaks observed between $2\theta = 10^\circ$ and 15° in Fig. 3(a) and at $\sim 15^\circ$ in Fig. 3(b) are due to the Mylar window of the sample holder [32].

Porosimetry analysis from adsorption/desorption isotherm provided the essential qualitative information as well as the estimation of quantitative properties of the porous structure of the ACs. The N_2 sorption isotherms of DS-AC in Fig. 4(a) exhibits a Type I isotherm nature as this AC contains majority of micropores. The N_2 adsorption increases sharply at low relative pressure (P/P_0) region and reaches a plateau in the higher relative pressure region suggest the microporosity nature of the AC [33]. The N_2 sorption isotherm of DSh-AC in Fig. 4(b) is showing a Type IV isotherm behaviour.

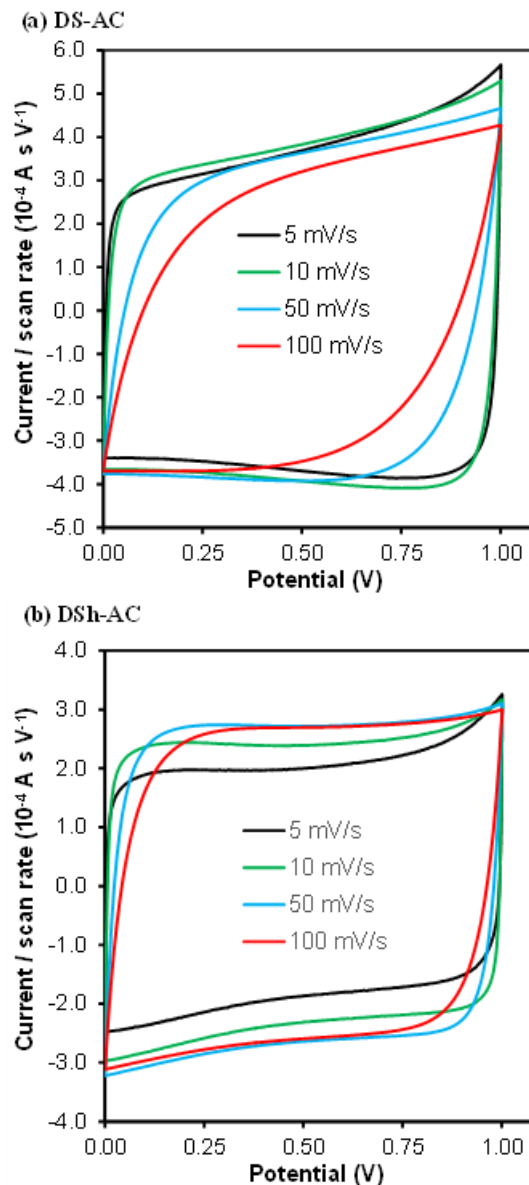


Figure 5. Cyclic voltammograms at scan rates of 5, 10, 50, and 100 $mV s^{-1}$ for EDLCs with (a) DS-AC and (b) DSh-AC as electrode material.

The inflection at $P/P_0 > 0.1$ suggests mesoporosity adsorption. Hysteresis loops of the isotherm is caused by the different mechanism of mesopores filling by capillary condensation during adsorption and desorption [33]. The porous properties given in Table 1 provide a quantitative summary of the porosity of DS-AC and DSh-AC which supports the deduced qualitative information from the isotherm patterns. The microporosity of DS-AC was shown by the high proportion of microporous surface area (S_{mic}) and microporous volume, (V_{mic}). The average pore width (D) of DS-AC at 1.93 nm is also in the micropores region which is less than 2.0 nm. As for the DSh-AC, S_{mic} and V_{mic} only account small proportion of BET surface area (S_{BET}) and total volume (V_t) respectively, which support-

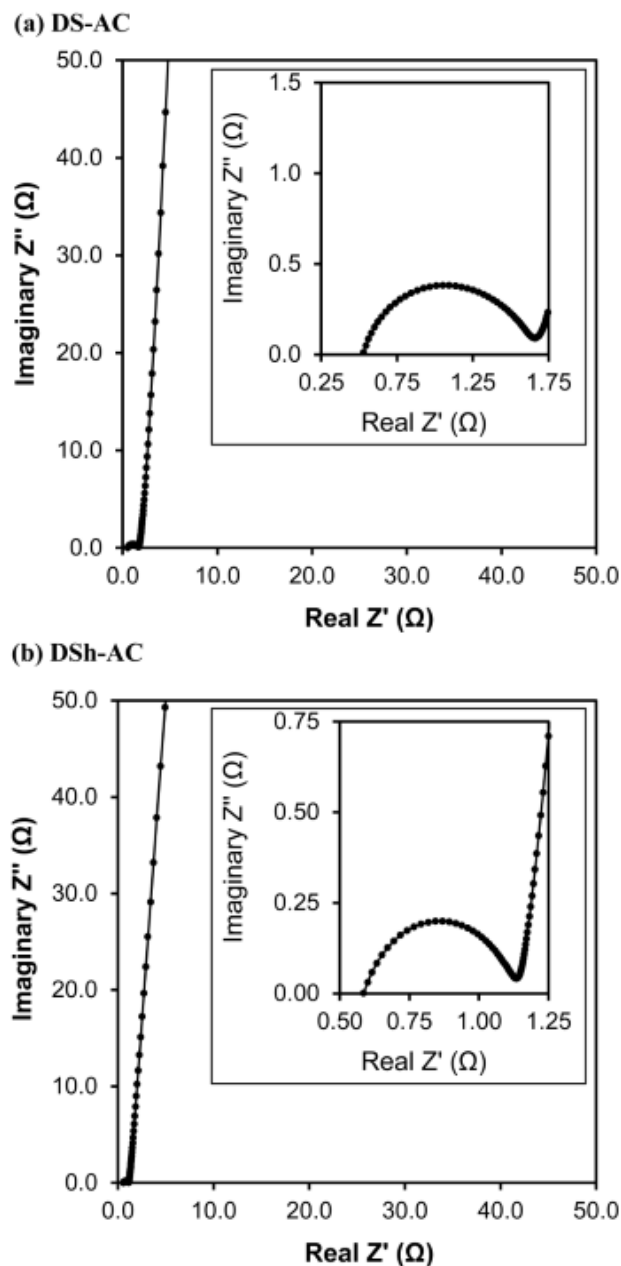


Figure 6. Nyquist plots of EDLC with (a) DS-AC and (b) DSh-AC as electrode materials. The insets show the expanded Nyquist plots in the high frequency region.

ed its mesoporosity. Its D of 3.34 nm shows that the pores are mesoporous. By comparison, DSh-AC has S_{BET} of 2004 m² g⁻¹ which is approximately double that of the DS-AC's S_{BET} .

3.2. Electrochemical properties of EDLC

Cyclic voltammograms for the EDLCs shown in Fig. 5 resemble fairly good parallelograms. An ideal capacitor shows a perfect rectangular voltammogram. The voltammogram of DS-AC based EDLC in Fig. 5(a) is having an increasing biconvex nature as the

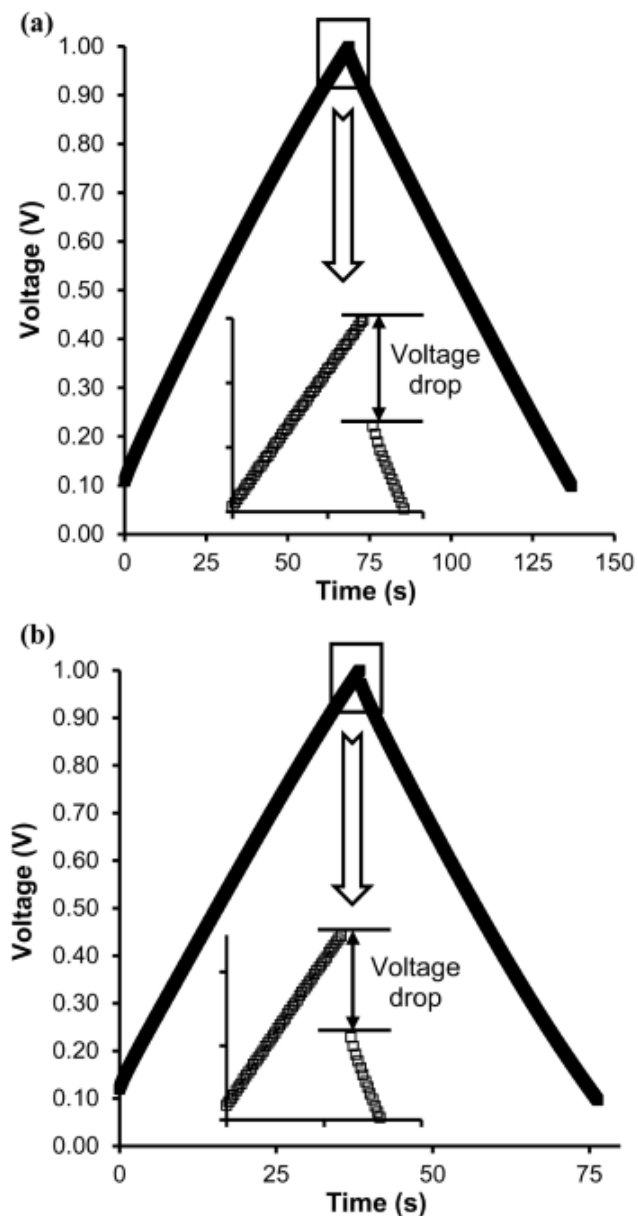


Figure 7. GCD curves of EDLC with (a) DS-AC and (b) DSh-AC as the electrode material at constant current of 5.0 mA. The inset in each figure is the voltage drop during the beginning of discharge.

scan rate increases. This phenomenon is due to the inability of charge movement to occupy available sites to catch up with the fast potential change [34]. It could be related to the high fraction of micropores in DS-AC which contributes to the resistance for the charge movement in the pores. DSh-AC based EDLC shows a more rectangular voltammogram even at higher scan rates. DSh-AC has a lower fraction of micropores and subsequently contributes to the lower resistive behavior of the pores. Here the charge occupancy of the available sites can take place quickly and reach a constant level regardless of the scan rate. The specific capacitance

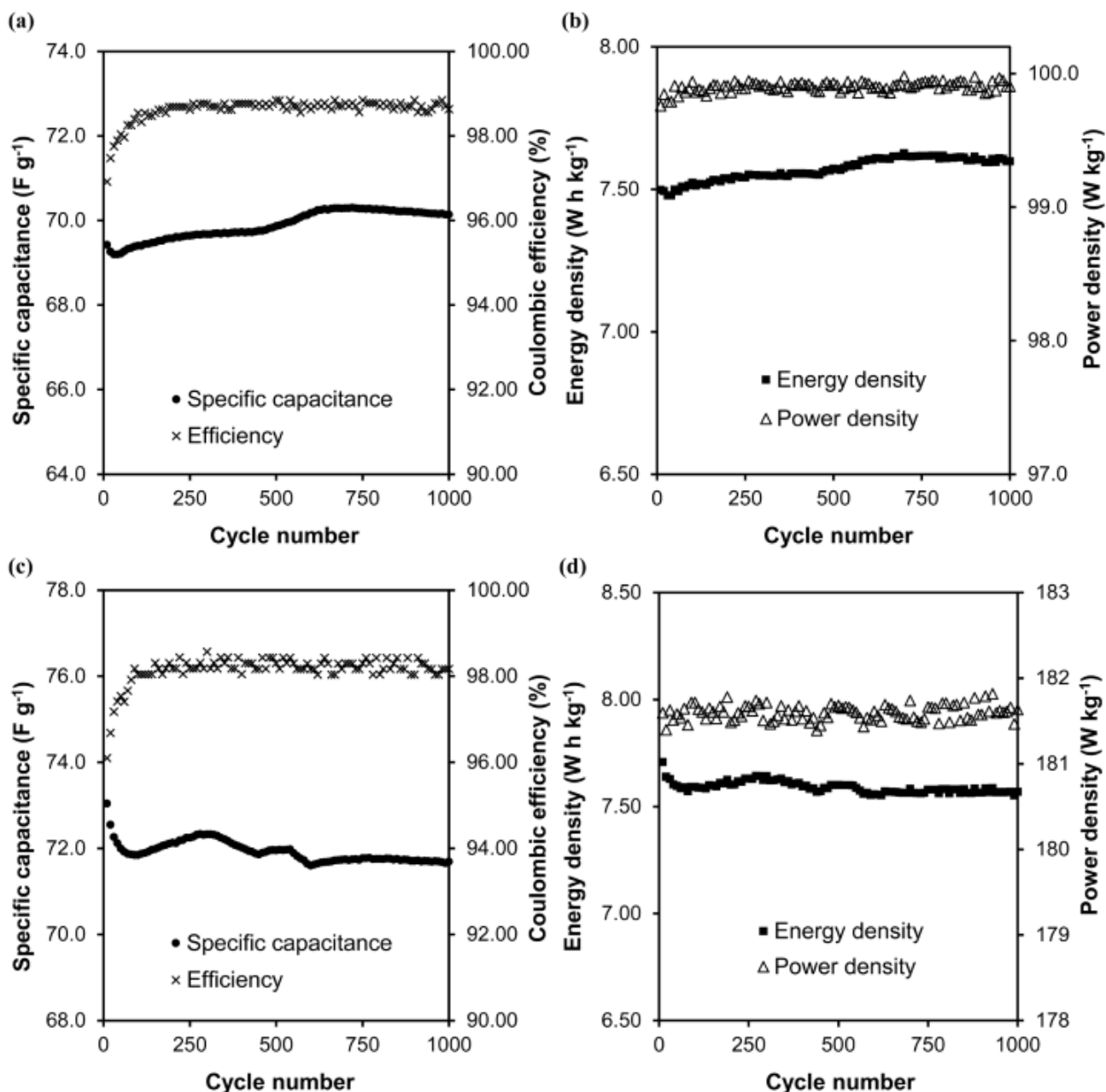


Figure 8. Plot of (a) specific capacitance and Coulombic efficiency, (b) energy density and power density for EDLC cell with DS-AC over 1000 cycles; plot of (c) specific capacitance and Coulombic efficiency, (d) energy density and power density for EDLC cell with DSh-AC over 1000 cycles.

of the AC material was calculated using the voltammogram of 50 mV s⁻¹. EDLCs of DS-AC and DSh-AC have specific capacitances (C_{SC}) of 64.8 and 82.5 F g⁻¹ respectively.

Electrochemical impedance spectroscopy (EIS) study can be used to explore the impedance behavior of the EDLC when an alternating voltage of different frequencies is applied to the capacitor. The Nyquist plots for both type of EDLCs are shown in Fig. 6. As seen from the Nyquist plots, both EDLCs have a semicircle in the high frequency region (>100 Hz). The first intercept on the real

axis at high frequencies corresponds to the bulk resistance (R_b) of the electrolyte and the second intercept of the semicircle corresponds to R_b+R_{ct} where R_{ct} is the charge transfer resistance at the electrolyte-electrode interface. The measured values of R_b are 0.52 and 0.59 Ω respectively for DS-AC and DSh-AC. While the EDLC cell of DS-AC has R_{ct} of 1.1 Ω , the EDLC with DSh-AC has R_{ct} of 0.54 Ω . Since the DS-AC has more micropores compared to DSh-AC, it shows a higher R_{ct} as expected. In the low frequency region, the capacitive behavior of the EDLC cells emerged as shown by the

nearly vertical line. Due to the electrical double layer, the line has a small deviation from the vertical line of an ideal capacitor. A summary of the impedance parameters for both EDLC cells are tabulated in Table 2.

The galvanostatic charge-discharge (GCD) involves ion adsorption and desorption at the electrode surfaces. The GCD curves obtained using constant current of 5 mA given in Fig. 7 show good linearity of voltage with time as expected for a good EDLC. By subjecting to a large number of charge-discharge cycles, the durability of the EDLCs were tested. Fig. 8 gives the variation of the four parameters (C_{sc} , Coulombic efficiency (η), energy density (E), and power density (P)) of both type of EDLCs with the cycle number over 1000 cycles. The efficiency of DS-AC based EDLC seems to be stabilized at approximately 98.72 % after 250 cycles of GCD. At the very beginning, the C_{sc} has the value of 69.4 F g⁻¹ and the value increases slightly and reaches a constant value of nearly 69.9 F g⁻¹. Energy density and power density are also quite stable across the GCD cycles, which are calculated to be around 7.59 Wh kg⁻¹ and 99.9 W kg⁻¹ respectively. As for the DSh-AC EDLC, stability is obtained after around 250 cycles of GCD with an efficiency of approximately 98.25 % and C_{sc} of 71.9 F g⁻¹. For this EDLC the energy density and power density are also stable with values of 7.58 Wh kg⁻¹ and 182 W kg⁻¹ respectively.

From previous reviews, while H₃PO₄ activated DS yielded S_{BET} of 2123 m² g⁻¹ [25], the KOH activated DSh yielded a maximum S_{BET} of 992 m² g⁻¹ [22]. It seems that H₃PO₄ can produce AC with higher S_{BET} as shown by the result obtained for DSh-AC in this work as well. Besides that, it has been reported that AC derived from banana fibers treated with zinc chloride had S_{BET} of 1100 m² g⁻¹ [35]. In this study, PVDF and NMP were used as the binder and solvent respectively for the coating of AC slurry onto nickel mesh. This EDLC with 1.0 M Na₂SO₄ electrolyte has produced C_{sc} of 74 F g⁻¹. However, its cyclic voltammograms were exhibiting biconvex nature especially at higher scan rates. In another reported study on bamboo based AC, activation with KOH yielded S_{BET} of 1300 m² g⁻¹ [36]. The highest C_{sc} achieved from this bamboo based EDLC was around 65 F g⁻¹ when used with sulfuric acid as electrolyte. Our specific capacity values are comparable to these reported results.

4. CONCLUSION

ACs were prepared by means of chemical activation from durian seeds (DS) and shells (DSh) as precursor materials. The DSh-AC had higher S_{BET} of 2004 m² g⁻¹ than that of the DS-AC of 1176 m² g⁻¹. It seems that the one-step phosphoric acid activation produces DS-AC with reasonable S_{BET} .

Although DSh-AC has minute amount of micropores, it still produces high values S_{BET} . When these ACs were used as electrode

material for EDLCs, DSh-AC produced better performance with average C_{sc} value ranging between 72 to 82 F g⁻¹. The cyclic voltammogram for the DSh-AC EDLC was very close to a perfect rectangle of an ideal capacitor even at higher scan rates. The charge transfer resistance R_{ct} of DSh-AC based EDLC has a relatively lower value compared to that of the DS-AC based EDLC and this is most probably due to the significantly small amount of the micropores in DSh-AC. Both type of EDLC cells were stable over 1000 cycles of GCD with efficiency staying above 98 %. DSh-AC electrode can achieve energy density and power density of 7.58 Wh kg⁻¹ and 182 W kg⁻¹ respectively.

The direct coating of AC slurry onto the GMF is a very straightforward method to prepare electrodes of EDLC cells without using polymer binders and organic solvents. AC slurry easily adhered to GMF because of its wettability. AC components get trapped in the spaces of GMF after the removal of water (solvent). GMF could also serve as a reservoir for liquid electrolytes and can have almost direct contact with the electrode materials.

Fossil fuel based carbon sources like coke, coal, and pitch are favourable precursors for AC due to their high carbon content. Due to the decreasing availability and detrimental environmental impact of fossil fuels, production of AC from renewable resources from nature such as agricultural wastes is being explored. DS and DSh are examples of such agricultural wastes. The promising capacitor performances reported above show that DS-AC and DSh-AC have good prospects to be among the major materials for EDLC fabrication.

5. ACKNOWLEDGEMENTS

This study is financially supported by University of Malaya Research Grant (UMRG) No. RG223-12AFR and Postgraduate Research Fund (PPP) No. PV094-2012A.

REFERENCES

- [1] Nossol E, Zarbin AJG, *Electrochim Acta*, 54, 582 (2008).
- [2] Konno H, Ito T, Ushiro M, Fushimi K, Azumi K., *J. Power Sources*, 195, 1739 (2010).
- [3] Jampani P, Manivannan A, Kumta PN, *Electrochem. Soc. Interface*, 19, 57 (2010).
- [4] Lota G, Centeno TA, Frackowiak E, Stoeckli F, *Electrochim. Acta*, 53, 2210 (2008).
- [5] Nandhini R, Mini PA, Avinash B, Nair SV, Subramanian KRV, *Mater. Lett.*, 87, 165 (2012).
- [6] Portet C, Taberna PL, Simon P, Flahaut E, Laberty-Robert C, *Electrochim. Acta*, 50, 4174 (2005).
- [7] Brousse T, Toupin M, Dugas R, Athouël L, Crosnier O, Bélanger D, *J. Electrochem. Soc.*, 153, 2171 (2006).
- [8] Feng L, Zhu Y, Ding H, Ni C, *J. Power Sources*, 267, 430 (2014).
- [9] Yin JL, Park JY, *Int. J. Hydrogen Energy*, 39, 16562 (2014).
- [10] Zhang LL, Wei T, Wang W, Zhao XS, *Microporous Mesoporous Mater.*, 123, 260 (2009).
- [11] Choi SH, Kim J, Yoon YS, *J. Power Sources*, 138, 360 (2004).
- [12] Yang J, Lan T, Liu J, Song Y, Wei M, *Electrochim. Acta*, 105, 489 (2013).

Table 2. Impedance parameters of EDLCs with DS-AC or DSh-AC as the electrode material.

EDLC cells	Bulk resistance, R_b (Ω)	Charge transfer resistance, R_{ct} (Ω)	Specific capacitance, C_{sc} (F g ⁻¹)
DS-AC	0.52	1.1	64.1
DSh-AC	0.59	0.54	77.3

- [13] Frackowiak E, Béguin F., *Carbon*, 39, 937 (2001).
- [14] Pandolfo AG, Hollenkamp AF, *J. Power Sources*, 157, 11 (2006).
- [15] Wei L, Yushin G., *Nano Energy*, 1, 552 (2012).
- [16] Chen Y, Huang B, Huang M, Cai B, *J. Taiwan Inst. Chem. Eng.*, 42, 837 (2011).
- [17] Daud WMAW, Ali WSW, *Bioresour. Technol.*, 93, 63 (2004).
- [18] Kalderis D, Bethanis S, Paraskeva P, Diamadopoulos E, *Bioresour. Technol.*, 99, 6809 (2008).
- [19] Lim WC, Srinivasakannan C, Balasubramanian N, *J. Anal. Appl. Pyrolysis*, 88, 181 (2010).
- [20] Ahmadpour A, Do DD, *Carbon*, 34, 471 (1996).
- [21] Sudaryanto Y, Hartono SB, Irawaty W, Hindarso H, Ismadji S, *Bioresour. Technol.*, 97, 734 (2006).
- [22] Chandra TC, Mirna MM, Sunarso J, Sudaryanto Y, Ismadji S, *J. Taiwan Inst. Chem. Eng.*, 40, 457 (2009).
- [23] Foo KY, Hameed BH, *Chem. Eng. J.*, 187, 53 (2012).
- [24] Nuithitikul K, Srikhun S, Hirunpraditkoon S, *Bioresour. Technol.*, 101, 426 (2010).
- [25] Ismal A, Sudrajat H, Jumbianti D, *Indones. J. of Chem.*, 10, 36 (2010).
- [26] Bicha t MP, Raymundo-Piñero E, Béguin F, *Carbon*, 48, 4351 (2010).
- [27] Demarconnay L, Raymundo-Piñero E, Béguin F, *Electrochem. Commun.*, 12, 1275 (2010).
- [28] Brown MJ. *Durio - A Bibliographic Review*. New Delhi, India: International Plant Genetic Resources Institute, 1997.
- [29] Hisham DMN, Lip JM, Suri R, Shafit HM, Kharis Z, Shazlin K, et al., *Eng. Technol.*, 69, 72 (2012).
- [30] Sing KSW, Everett DH, Haul R, Moscou L, Pierotti RA, Rouquerol J, et al., *Pure Appl. Chem.*, 57, 603 (1985).
- [31] Ryu Z, Rong H, Zheng J, Wang M, Zhang B, *Carbon*, 40, 1144 (2002).
- [32] Kafunkova E, Lang K, Kubat P, Klementova M, Mosinger J, Slouf M, et al., *J. Mater. Chem.*, 20, 9423 (2010).
- [33] Marsh H, Reinoso, *Activated Carbon*. Amsterdam London: Elsevier; 2006.
- [34] Fletcher S, Black V, Kirkpatrick I, *J. Solid State Electrochem.*, 18, 1377 (2014).
- [35] Subramanian V, Luo C, Stephan AM, Nahm KS, Thomas S, Wei B, *J. Phys. Chem. C*, 111, 7527 (2007).
- [36] Kim Y-J, Lee B-J, Suezaki H, Chino T, Abe Y, Yanagiura T, et al., *Carbon*, 44, 1592 (2006).